Lipopolysaccharides of *Campylobacter jejuni* Serotype O:19: Structures of Core Oligosaccharide Regions from the Serostrain and Two Bacterial Isolates from Patients with the Guillain–Barré Syndrome†

Gerald O. Aspinall,*,‡ Armando G. McDonald,‡ Henrianna Pang,§ Linda A. Kurjanczyk,∥ and John L. Penner∥

Department of Chemistry, York University, North York, Toronto, Ontario M3J 1P3, Canada, and Carbohydrate Research Centre, Department of Molecular and Medical Genetics, and Department of Microbiology, University of Toronto, Toronto, Ontario M5S 1A8, Canada

Received July 1, 1993; Revised Manuscript Received October 7, 1993⊗

ABSTRACT: Lipopolysaccharides from phenol–water extraction of cells of *Campylobacter jejuni* serotype O:19 were separated into a water-soluble gel of low M_r and a water-soluble component of high M_r. Acetic acid hydrolysis of the ketosidic linkages to lipid A furnished respectively a core oligosaccharide, the structure of which is reported herein, and an O antigenic polysaccharide. Structural investigations were performed on the *O*-deacetylated lipopolysaccharide of low M_r, the liberated core oligosaccharide and the various products from removal of neuraminic acid and phosphate residues, and from the Smith degradation. It is concluded that the lipopolysaccharide from the serostrain has a core region with two types of closely related oligosaccharide chains showing striking homologies with gangliosides, the first with a single *N*-acetylneuraminic acid residue in an outer chain resembling GM_1 and the second with two *N*-acetylneuraminic acid residues with a terminal region resembling GD_{1a}. Similar experiments were carried out on lipopolysaccharides of low M_r from bacterial isolates OH 4384 and OH 4382 serotyped as O:19 that had been obtained from two patients who subsequently developed the Guillain–Barré syndrome. The core oligosaccharide region of lipopolysaccharide from the former isolate differed only slightly from that of the serostrain, whereas that from the latter isolate was distinctly shorter.

The Guillain–Barré syndrome (GBS),[1] although of relatively infrequent occurrence, is the most common cause of acute generalized paralysis (Ropper, 1992). One of the best documented conditions associated with the subsequent onset of GBS is that of previous *Campylobacter jejuni* infection. An interesting aspect of this association is the correlation of elevation of anti-ganglioside GM_1 antibodies with the severity of the symptoms (Walsh et al. 1991). The significance of this observation became more apparent with the demonstration that regions of LPS from *C. jejuni* serotype O:4 (Aspinall et al., 1992, 1993b) were homologous with those of monosialo- (GM_1) and disialo- (GD_{1a}) gangliosides. The discovery, by the passive hemagglutination assay (Penner et al., 1983), that in Japan over 90% of cases of GBS which had been preceded by a bout of diarrhea from *Campylobacter* infections were due to *C. jejuni* serotype O:19 was of particular interest (Kuroki et al., 1991). It has also been demonstrated that IgM antibodies against ganglioside GM_1 occur in GBS patient sera after *C. jejuni* infection (Yuki et al., 1990). These observations prompted an examination of the detailed structure of the LPS from the O:19 serotype for comparison with those of other serotypes to gain possible insight into the mechanisms of pathogenesis.

In results reported elsewhere (Aspinall et al., 1993a), electrophoretic examination by SDS–PAGE of LPS from serostrains of *C. jejuni* O:4 and O:19 showed the presence of cross-reacting low M_r LPS and of high M_r LPS in series of bands indicating incremental additions of O chain repeating units but with different spacings for the two serotypes. The results pointed to common epitopes in the core OS regions but with different O antigen chains, a conclusion supported by detection of the high M_r components with homologous but not with heterologous antisera.

LPS samples were also obtained from two O:19 typed isolates, designated OH 4382 and OH 4384 (S. Fujimoto, personal communication), that had been obtained from two siblings infected with *C. jejuni* within a 10-day period and who were both subsequently diagnosed with GBS. Examination of these samples by SDS–PAGE in comparison with that from the O:19 serostrain showed cross-reactions of both low and high M_r LPS components. The low M_r LPS from OH 4382 was of higher mobility and presumably of shorter chain length than that from the type strain, but that from OH 4384 was less markedly different. The high M_r LPS samples showed bands displaced with respect to that of the serostrain but with similar spacings. The results were suggestive of LPS samples from the two O:19 typed isolates with similar O chain repeating units attached to nonidentical core regions.

† This work was supported by strategic and operating grants from the Natural Sciences and Engineering Research Council of Canada (to G.O.A.) and the Medical Research Council of Canada (for the Carbohydrate Research Centre).

* Address correspondence to this author.

‡ York University.

§ Carbohydrate Research Centre, University of Toronto.

∥ Department of Microbiology, University of Toronto

⊗ Abstract published in *Advance ACS Abstracts,* December 1, 1993.

[1] Abbreviations: 1D, one-dimensional; 2D, two-dimensional; CI, chemical ionization; COSY, correlated spectroscopy; EI, electron impact; FAB/MS, fast atom bombardment mass spectrometry; Gal, galactose; GalNAc, *N*-acetylgalactosamine; GBS, Guillain–Barré syndrome: GC/MS, gas chromatography–mass spectrometry; Glc, glucose; GPC, gel-permeation chromatography; Hep, heptose; LD-Hep, L-*glycero*-D-*manno*-heptose; 3-dHexitol, 3-deoxyhexitol; HF, hydrofluoric acid; KDO, 3-deoxy-D-*manno*-octulosonic acid; LPS, lipopolysaccharide; Man, mannose; Neu5Ac, *N*-acetylneuraminic acid; NMR, nuclear magnetic resonance; OS, oligosaccharide; PAGE, polyacrylamide gel electrophoresis; PEA, *O*-phosphoethanolamine; RCT, relay coherence transfer; SDS, sodium dodecyl sulfate.

0006-2960/94/0433-241$04.50/0

In this paper we report structural studies on LPS samples which (a) establish the relationship of the low M_r component from the *C. jejuni* O:19 serostrain to that of *C. jejuni* O:4 and (b) define the differences in the corresponding lipopolysaccharides of low M_r from the typed isolates from GBS patients. The accompanying paper (Aspinall et al., 1994) reports investigations which elucidate the detailed structure of identical O antigen chains in the various O:19 high M_r LPS samples.

EXPERIMENTAL PROCEDURES

Isolation of Lipopolysaccharides, O-Deacylated Lipopolysaccharide (OS 19-C1), Liberated Core Oligosaccharide (OS 19-C2), and Antigenic Polysaccharide (PS 19-P1). Bacterial culture conditions were those previously described (Penner & Hennessy, 1980), and bacterial cells were extracted by the phenol–water method (Westphal & Jann, 1965). The aqueous layer was removed, dialyzed for 48 h against distilled water, and ultracentrifuged (100000*g* for 4 h). A portion of the gel-like pellet that separated was treated with anhydrous hydrazine at 40 °C for 1 h to yield *O*-deacylated lipopolysaccharide OS **19**-C1. The remainder of the gel-like pellet was hydrolyzed in aqueous 1% acetic acid for 1 h at 100 °C. Insoluble lipid A was removed by centrifugation. The water-soluble material was fractionated by GPC on Bio-Gel P-2 (1 × 100 cm) and water elution yielded OS **19**-C2. The supernatant liquid from the ultracentrifugation was treated likewise, lipid A was removed by centrifugation, and the water-soluble material was fractionated by GPC on Bio-Gel P-6 (1.1 × 110 cm) and eluted with water to yield polysaccharide (PS **19**-P1) at the void volume. GPC fractions (~1 mL) were collected, assayed by phenol–sulfuric acid for carbohydrate (Dubois et al., 1956), and pooled.

The same procedure was used later for the isolation of LPS samples from bacterial isolates OH 4382 and OH 4384 that had been typed as O:19.

^1H and ^{13}C Spectroscopy. One-dimensional (1D) and two-dimensional (2D) experiments were performed on a Bruker AM 300 spectrometer in the Fourier transform mode. Oligosaccharide samples were exchanged (three times) with D_2O (99.99%). ^1H NMR spectra and proton homonuclear 2D COSY and COSY-RCT experiments were recorded using a 5-mm probe at 25 °C, and chemical shifts were measured relative to acetone (δ 2.225). ^{13}C NMR spectra were obtained using variously (i) broad-band decoupled (ii) proton coupled, and (iii) *J*-modulated ^1H–^{13}C spin echo experiments at 25 °C. Chemical shifts were measured relative to internal acetone (δ 31.4). The ^{31}P NMR spectra were recorded using a 10-mm broad-band probe at 25 °C and chemical shifts were measured relative to external orthophosphoric acid (δ 0.0). All experiments were performed with standard Bruker software.

Methylations. Oligosaccharides (~0.4 mg) were methylated in Me_2SO by the method of Ciucanu and Kerek (1984). *O*-Deacylated LPS were methylated in Me_2SO with isolation by passage through Sep-Pak C_{18} cartridges (York et al., 1986). Permethylated derivatives were hydrolyzed in aqueous 4 M trifluoroacetic acid for 6 h at 100 °C, the products were reduced with $NaBD_4$ and acetylated, and partially methylated alditol acetates were analyzed by GC/MS using programs B and C.

Chemical Modifications of Oligosaccharides and the Smith Degradation. Complete removal of Neu5Ac residues from oligosaccharides was achieved by mild hydrolysis in aqueous 2 M acetic acid at 80 °C for 16 h. *O*-Dephosphorylations were carried out by treatment with aqueous 48% HF at 4 °C for 72 h. Excess acid was removed in a vacuum desiccator over KOH. Oligosaccharides from these treatments were purified by GPC on Bio-Gel P-2 (1.0 × 100 cm). For the preparation of OS **19**-C3, OS **19**-C2 was first dephosphorylated and and then desialylated. For the Smith degradation, OS **19**-C2 (~9 mg) was prereduced with $NaBD_4$ and then dephosphorylated to give OS **19**-C4. OS **19**-C4 was successively oxidized with $NaIO_4$, as described by Pritchard et al. (1988), desalted by GPC on Bio-Gel P-2, reduced with $NaBD_4$, decationized and concentrated with methanol, hydrolyzed with 1 M CF_3CO_2H at 45 °C for 1 h, and again reduced with $NaBD_4$ as before to give two oligosaccharide fractions, OS **19**-C4 (1.2 mg) and OS **19**-C5 (0.9 mg).

Analytical and Spectroscopic Methods. GC was performed on a Hewlett-Parkard Model 5890 chromatograph. Separations were carried out using capillary columns with the following programs: (A) DB-23 (15 m × 0.5 mm or 30 m × 0.25 mm) isothermally at 220 °C; (B) DB-17 (15 m × 0.25 mm) isothermally at 190 °C; (C) DB-23 (30 m × 0.25 mm) isothermally at 190 °C; (D) DB-23 (30 m × 0.25 mm) at 200 °C (10 min), 200–240 °C at 2 °C/min, and 240 °C (20 min); (E) DB-17 (15 m × 0.25 mm) at 50 °C (5 min) and 50–100 °C at 2 °/min; (F) DB-5 (15 m × 0.25 mm) from 150 to 250 °C at 2 °C/min. GC/MS was performed using a Kratos Analytical Profile instrument in the EI (70 eV, source temperature 220 °C) and CI (ammonia reagent gas, source temperature 180 °C) modes, equipped with a Hewlett-Packard Model 5890 chromatograph, and using the above GC programs.

FAB/MS were recorded with a VGZAB-SE instrument equipped with an Ion Tech saddle field gun. Permethylated samples in methanol (1–2 μL) were loaded onto the target with a matrix (1 μL) of thioglycerol of 3:1 thioglycerol–glycerol. Samples were bombarded with xenon atoms (1.2 mA anode current, 8 keV anode potential), spectra were recorded with a VG 11-250 data system under the multichannel analyzing mode, and 4–5 scans were acquired. Resolution was set at 1500–2000 (10% valley definition), and CsI was used as the calibrant. In some cases, the resolution was set lower in the high mass range; hence, the average mass to charge was observed for the molecular ion. For accurate mass measurements, resolution was set at 10 000, a narrow mass range was scanned using the accelerating voltage, and 2% poly(ethylene glycol) was included in the matrix as internal calibrant. All molecular ions and fragment ions are reported as the nominal mass of the ^{12}C-containing component (corresponding to the mass of integral atomic weights). The observed mass is about 1.5 amu higher in the 2000 mass range.

Interpretations of positive ion mass spectra of permethylated derivatives were as described by Dell et al. (1990) and used in earlier publications (Aspinall et al., 1993b). Spectra of methylated derivatives from OS with reducing KDO termini showed that the major component of the molecular ion cluster corresponded to that calculated for $[M + H]^+$ or other adduct ions. Related ions at $([M + H]^+ - 46)$ and $([M + H]^+ - 116)$, with structures arising from degradation at the KDO termini as proposed by Deli et al. (1990), were sometimes seen and their co-occurrence with those at $[M + H]^+$ aided in the identification of molecular ions. In the case of OS bearing PEA moieties, the main components of the molecular ion cluster corresponded to molecular cations designated as $[MCH_3]^+$ with the covalently linked $-CH_2-CH_2-N(CH_3)_3^+$ group formed from the PEA moiety and thus not requiring further protonation. The postulation of charged permethylated derivatives also served to explain the absence of glycosyloxonium fragment ions arising from cleavage of glycosidic linkages at the inner PEA-bearing heptopyranosyl residues.

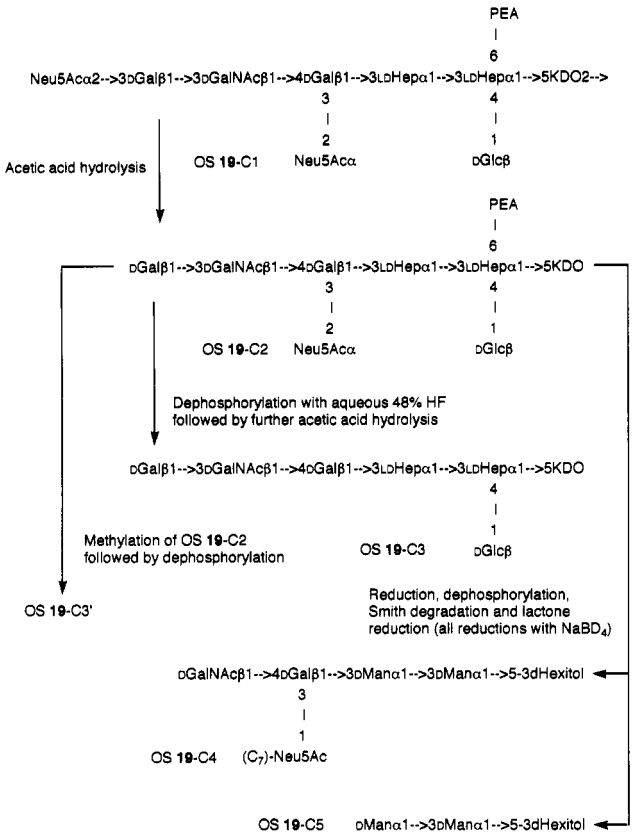

FIGURE 1: Genesis of OS **19** fractions from *C. jejuni* O:19 LPS, where structure OS **19**-C1 represents the most extended core OS chain in the intact LPS.

The corresponding fragment ions were observed from cleavage at residues bearing phosphomonoester (P) substituents.

Other Analytical Procedures. Glycose analyses as alditol acetate derivatives (Sawardeker et al., 1967) were performed by GC using program A. Enantiomeric configurations were established by conversion of aldoses into 2-(*R*)- and 2-(*S*)-butyl glycosides (Gerwig et al., 1978) and GC analysis of acetylated derivatives using program D. The identities of KDO and Neu5Ac derivatives in core OS, *O*-deacylated LPS, and their permethylated derivatives were established by methanolysis (0.75 M CF_3CO_2H at 100 °C for 6 h), followed by acetylation and GC/MS analysis using program F. Phosphate analyses were performed by the method of Chen et al. (1956).

RESULTS

Isolation of Lipopolysaccharide of Low M_r and the Derived Core Oligosaccharide. Lipopolysaccharide of low M_r was isolated as a gel-like pellet by ultracentrifugation of the aqueous layer from the phenol–water extraction. The immunological cross-reaction of this LPS with that from *C. jejuni* serotype O:4 suggested that Neu5Ac residues might be present and therefore be inadvertently lost during the liberation of core oligosaccharide from lipid A by mild acid hydrolysis. The overall strategy adopted in the characterization of the core oligosaccharide region of the LPS was based on experience gained in studies on the O:4 LPS and is summarized in Figure 1. Compositional and structural information was obtained from studies on the otherwise intact *O*-deacylated LPS (for which structure OS **19**-C1 represents the most extended core OS in the intact LPS) as well as on the liberated core OS **19**-C2 and the derivative, OS **19**-C3, from subsequent *O*-dephosphorylation with aqueous 48% HF and further hydrolysis for complete liberation of Neu5Ac residues. Hydrolysis of the core OS **19**-C2 gave Glc, Gal, GalNAc, and LD-Hep, analyzed as alditol acetates, in the approximate ratio of 1:2:0.4:1. In our experience analysis for HexNAc commonly gives low values and incomplete liberation of LD-Hep frequently occurs if *O*-phosphoethanolamine (PEA) substituents are present (Moran et al., 1991). Hydrolysis of OS **19**-C3, after *O*-dephosphorylation, yielded double the quantity of LD-Hep. All sugars had the D ring configuration as determined through the formation of acetylated (*S*)- or (*R*)-2-butyl glycosides (Gerwig et al., 1978). Qualitatively, the presence of KDO and Neu5Ac was established through the formation of methyl ester methyl ketosides. Phosphate analysis showed the presence of approximately 1 residue per oligosaccharide chain of 8–9 residues. A more precise estimate of overall composition was obtained later from FAB/MS data.

Table 1: Methylation Analysis of Core Oligosaccharides from *C. jejuni* O:19 LPS

	molar ratios in oligosaccharides[a]					
methylated sugar	OS 19-C1	OS 19-C2	OS 19-C3	OS 19-C3′	OS 19-C4	OS 19-C5
2,3,4,6-Me_4-Glc	1.4	1.1	0.6	0.8		
2,3,4,6-Me_4-Gal	0.7	1.1	0.8	0.8		0.05
2,3,4,6-Me_4-Man						1.4
2,3,6-Me_3-Gal	0.5		1.1	1.5	0.8	
2,4,6-Me_3-Gal	0.7					
2,6-Me_2-Gal	1.4	1.4		0.4		
2,4,6-Me_3-Man					2.0	1.0
2,4,6,7-Me_4-Hep	1.0	1.0	1.0	1.0		
2,6,7-Me_3-Hep			1.0			
2,7-Me_2-Hep				1.0		
2,6-Me_2-Hep				0.7		
3,4,6-Me_3-GalNAc					0.4	
4,6-Me_2-GalNAc	0.3	0.5	0.3	0.3		
1,2,4,6-Me_4-3-dHexitol					0.3	tr
4,7,8,9-Me_4-Neu5Ac[c]	+	+				

[a] Molar ratios are based on relative peak areas in GC/MS analyses of partially methylated alditol acetates and are normalized with respect to Hep or Man residues. [b] 3-dHexitol, 3-deoxyhexitol. [c] Neu5Ac derivatives were identified by GC/MS of methyl ester methyl glycosides.

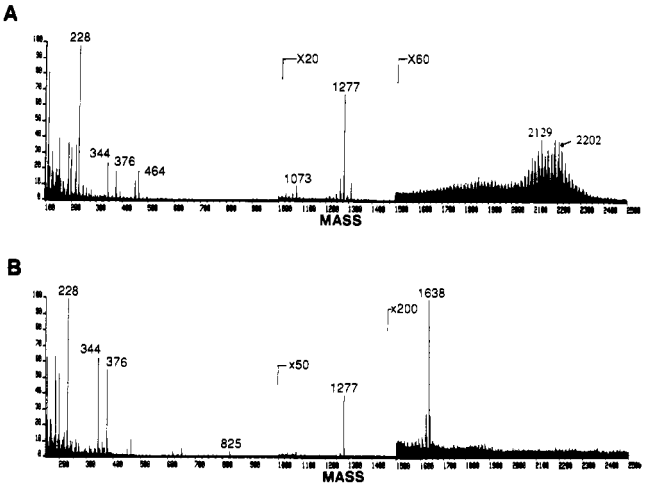

FIGURE 2: Positive ion FAB/MS spectrum of permethylated (A) OS **19**-C2 and (B) OS **19**-C1.

Linkage and Sequence Determination for the Core Oligosaccharide Region of C. jejuni Serotype O:19 Lipopolysaccharide. The first detailed information on the structure of the oligosaccharide region came from linkage analysis of the permethylated liberated core oligosaccharide OS **19**-C2 (Table 1), which may be considered together with the FAB/MS for this derivative (Figures 2 and 3). Ions at m/z 2202 ($[MCH_3]^+$) and 2156 ($[MCH_3]^+ - 46$) corresponded to a composition of

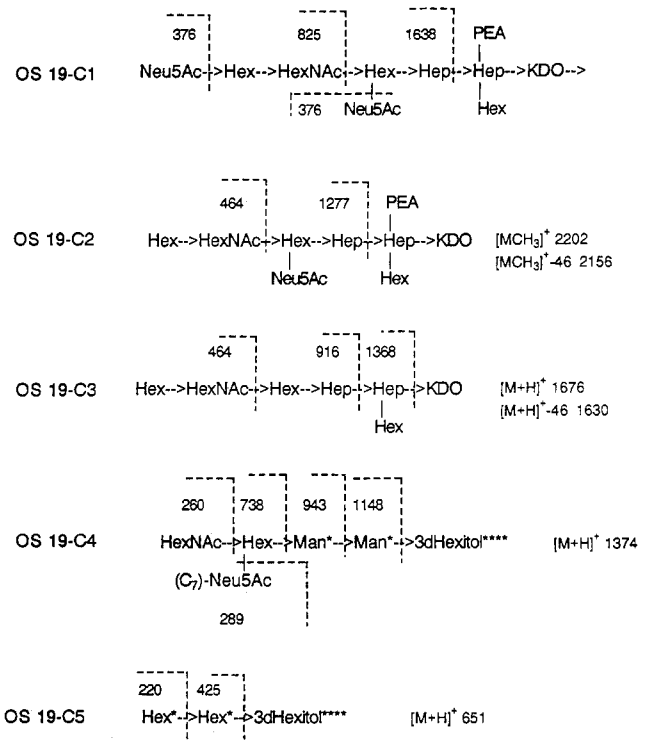

FIGURE 3: Analysis of positive ion FAB/MS data for permethylated core region in LPS from *C. jejuni* serotype O:19 and permethylated core OS derivatives. 3-dHexitol = 3-deoxyhexitol. Asterisks show incorporation of ^2H isotope.

Neu5Ac Hex_3 Hep_2 HexNAc PEA KDO. Fragment ions at m/z 376 (Neu5Ac), 464 (Hex HexNAc), and 1277 (Neu5Ac Hex_2 HexNAc Hep) (Figure 2A) with none detectable at intermediate mass indicated a branched structure for the terminal segment with a Gal residue bearing a Neu5Ac residue as a lateral side chain in the partial structure [Hex-HexNAc-Gal(Neu5Ac)-Hep]. With typically incomplete liberation of Hep on hydrolysis of residues with attached PEA units and in the absence of fragment ions from mass spectral cleavage in this region, the inner structure remained undefined. These aspects of structure together with evidence for the site of attachment of the lateral Neu5Ac residue were resolved from the linkage analysis (Table I) and accompanying FAB/MS for permethylated OS **19**-C3 after *O*-dephosphorylation and mild acid hydrolysis to remove the remaining Neu5Ac residue. FAB/MS data (Figure 3) showing fragment ions at m/z 464, 668, 916, and 1368 defined the linear sequence up to the inner branched Hep residue. Linkage analysis showed that the newly exposed 4-linked Gal residue has formerly borne the Neu5Ac residue at O-3 and that the inner 3,4-branched Hep residue carried a Hex side chain, but linkages at that branch point and the site of attachment to the reducing-terminal KDO remained to be determined. Linkage analysis of the product (OS **19**-C3′) from *O*-dephosphorylation of permethylated Os **19**-C2 gave *inter alia* a mixture of 3,4,6- and 3,4,7-tri-*O*-substituted LD-Hep derivatives showing that the PEA moiety had been located at O-6 mainly, but to a lesser extent at O-7, of the inner Hep residue.

Evidence for the presence of a second Neu5Ac residue in the native LPS was obtained from linkage analysis (Table I) and FAB/MS (Figures 2B and 3) of the permethylated derivative formed from the *O*-deacylated LPS OS **19**-C1. Linkage analysis showed that approximately half of the terminal Gal residues in liberated core OS **19**-C2 carried Neu5Ac residues at O-3 in the LPS. Fragment ions in permethylated OS **19**-C1 at m/z 825 and 1638 in addition to those at m/z 464 and 1277 were in accord with the presence of two chains, one with two Neu5Ac residues as in the ganglioside GD_{1a} and the other with only one Neu5Ac residue in lateral attachment as in GM_1. These results also implied that the terminal Glc residue is that linked to the inner Hep residue.

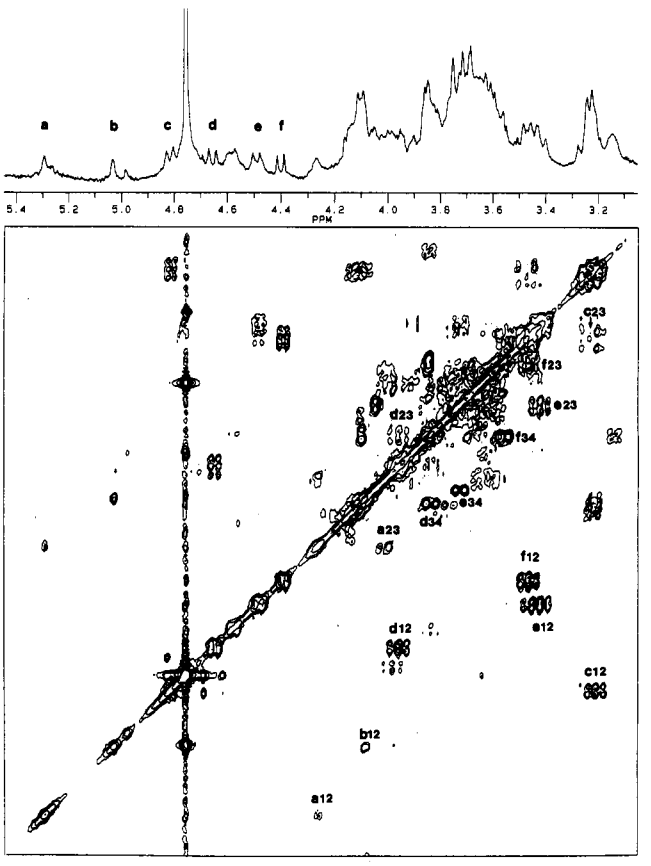

FIGURE 4: ^1H–^1H COSY spectrum (300 MHz) of OS **19**-C2.

NMR Spectroscopy and Configurational Assignments in OS 19-C2. ^1H NMR data showed the presence of OS **19**-C2 of six anomeric proton resonances, two three-proton singlets at δ 2.08 and 2.07 that could be assigned to *N*-acetyl substituents of GalNAc and Neu5Ac residues, and a signal at δ 2.70 (dd, 11 and 3 Hz) assigned to H-3 (equatorial) of Neu5Ac. These features were also apparent in the ^{13}C NMR spectrum for OS **19**-C2 which showed *inter alia* signals at δ 23.8 and 23.2 for methyl carbons (CH_3CO) and at δ 176.2 (double intensity), 175.9, and 175.1, assignable to carbonyl groups of the two *N*-acetyl substituents and the two carboxyl groups of Neu5Ac and KDO. A methylene signal at δ 41.2 ($J_{CP} \sim 7$ Hz) was assigned to the CH_2NH_2 of the PEA group. The anomeric proton resonances were characteristic of those from four residues with *β-galacto* or *β-gluco* ring configurations and two residues with *α-manno* ring configurations found in LD-Hep residues. Partial proton resonance assignments from 2D COSY (Figure 4) and COSY-RCT experiments enabled ring configurations for each of the residues to be determined and the results are summarized in Table 2. Two anomeric resonances at δ 5.36 and 5.09 (both broad singlets) associated with low $J_{2,3}$ values of $\sim$2 Hz were assigned to LD-Hep residues. Connectivities of the three anomeric resonances at δ 4.71, 4.55, and 4.46 having $J_{1,2}$ values of 7–8 Hz with those of H-3 and H-4 with low $J_{3,4}$ and $J_{4,5}$ values allowed the *β-galacto* configuration to be assigned to these Gal or GalNAc residues. In parallel fashion the anomeric resonance at δ 4.88 was assigned to a β-Glc residue.

Table 2: ^{1}H NMR Chemical Shift Data (ppm) for OS **19**-C2[a]

residue[b]	assigned configuration	H-1 ($J_{1,2}$)	H-2 ($J_{2,3}$)	H-3 ($J_{3,4}$)	H-4 ($J_{4,5}$)
a	α-Man	5.36 (br s)	4.33 (~2)	4.08 (~8)	
b	α-Man	5.09 (br s)	4.13 (~2)		
c	β-Glc	4.86 (7.7)	3.29 (~8)	3.52 (~8)	
d	β-Gal (or GalNAc)	4.71 (8.4)	4.01 (~8)	3.91 (~3)	4.17 (~3)
e	β-Gal (or GalNAc)	4.55 (7.8)	3.46 (~8)	3.79 (~3)	4.13 (~3)
f	β-Gal (or GalNAc)	4.46 (7.5)	3.52 (~8)	3.63 (~3)	3.92 (~3)

[a] Coupling constants are given in parentheses (in hertz). $J_{1,2}$ values were obtained from 1D spectra; other values were from COSY and COSY-RCT spectra. [b] Residues a–f as in Figure 4.

Smith Degradation and the Resolution of Linkage Ambiguities. From inspection of the structural units revealed by linkage analysis and the sugar sequences indicated from the FAB-MS data, it was clear that (a) the incompletely defined Hep and KDO residues would be resistant to endocyclic cleavage on oxidation with periodate and (b) that hexose end groups would be removed in a Smith degradation (Goldstein et al., 1965). Since exocyclic cleavage was anticipated in LD-Hep, Neu5Ac, and KDO residues, oxidation products were treated with $NaBD_4$ to stabilize and label the resulting modified units. In order to form a recognizable product from the KDO moiety (Aspinall et al., 1993b), the Smith degradation was performed on OS **19**-C2 after reduction ($NaBD_4$) and *O*-dephosphorylation. The sequence of reactions of oxidation, reduction ($NaBD_4$), and hydrolysis of acyclic acetals accompanied by lactonization was followed by a further reduction ($NaBD_4$) to yield a hexasaccharide, OS **19**-C4, and a trisaccharide, OS **19**-C5. FAB/MS data (Figure 3) together with linkage analysis of methylated derivatives showed that both oligosaccharides were terminated by 5-Ac-3-deoxy-1,2,4,6-Me_4-[$^2H_4$]hexitol residues that originated from a 5-linked KDO terminus. Linkage analysis showed trisaccharide OS **19**-C5 to contain two [$^2H_1$]Man residues arising from the Hep residues, joined by a 1→3 linkage, and with the same 3-dHexitol terminus as in OS **19**-C4. The formation of this trisaccharide presumably results from hydrolytic removal of Neu5Ac residues during the *O*-dephosphorylation with aqueous HF and consequent exposure of the Gal residue to periodate oxidation in the Smith degradation. The hexasaccharide OS **19**-C4 was shown by linkage analysis and FAB/MS to possess the more extended structure with the same modified "reducing" terminus, loss of non-reducing-terminal Gal and Glc residues, and attenuation of the lateral Neu5Ac residue to its 5-acetamido-3,5-dideoxy-7-[$^2H_1$]heptulosonic acid analog. In confirmation of earlier assignments, ^{1}H NMR data for OS **19**-C5 showed the presence of two broad singlets at δ 5.15 and 5.07, typical of anomeric resonances of α-Man residues. Similarly, ^{1}H NMR data for OS **19**-C4 showed resonances attributable to two α-Man residues at δ 5.20 and 5.07 and to two residues (Gal and GalNAc) with the *β-galacto* configuration at δ 4.81 ($J_{1,2}$ 8.0 Hz) and 4.61 ($J_{1,2}$ 7.9 Hz), together with two three-proton singlets at δ 2.06 and 2.03 for *N*-acetyl groups of GalNAc and modified Neu5Ac residues.

Lipopolysaccharides of Low M_r from O:19 Typed Isolates OH 4382 and OH 4384. Lipopolysaccharides of low M_r were isolated from phenol–water extractions of bacterial cells from isolates obtained from two diagnosed GBS patients of the same family, both of whom had been previously infected with *C. jejuni* strains serotyped as O:19. Since SDS–PAGE had shown lack of complete identity between LPS samples from the two bacterial isolates, as well as lack of identity to the serostrain, LPS of both high and low M_r were prepared separately from the isolates. Samples of *O*-deacylated LPS,

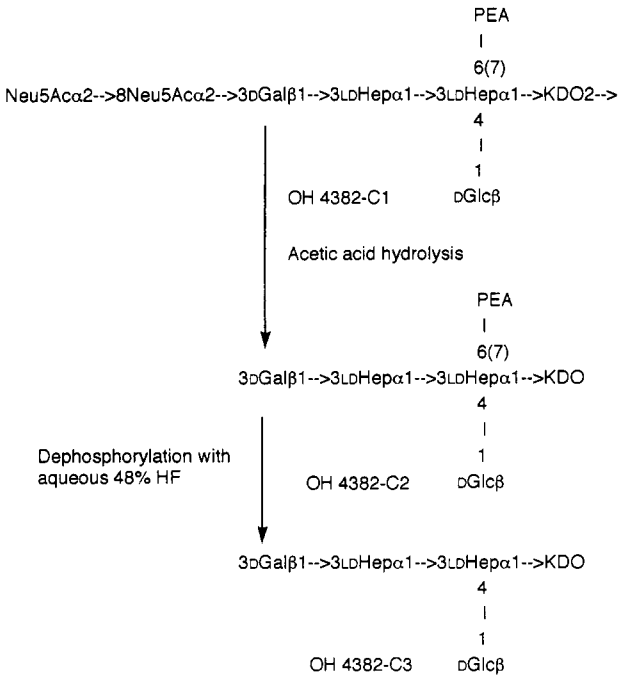

FIGURE 5: Genesis of fractions from LPS of isolate OH 4382, where structure OH 4382-C1 represents the most extended core OS chain in the intact LPS.

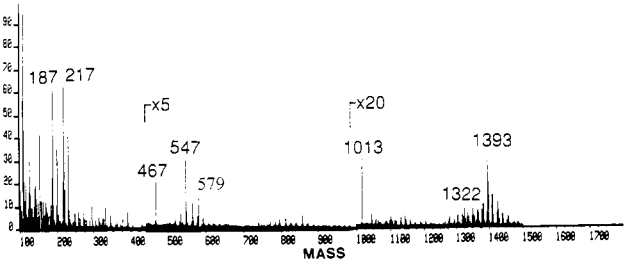

FIGURE 6: Positive ion FAB/MS spectrum of permethylated OH 4382-C2.

liberated core oligosaccharides, and their derivatives were prepared from LPS of low M_r, as described previously for the O:19 serostrain. The available quantities of LPS from the two isolates did not permit examinations as detailed as for the type strain but were sufficient to determine the structural relationships between the LPS samples.

O-Deacylated LPS from Isolate OH 4382, Core Oligosaccharide, and Derivatives. The conclusions from structural investigations on the *O*-deacylated LPS (designated as OH 4382-C1), the liberated OH 4382-C2, and the *O*-dephosphorylated derivative OH 4382-C3 formed on treatment with aqueous 48% HF are summarized in the partial structures shown in Figure 5. Compositional analysis showed that the LPS contained residues of Glc, Gal, Hep (all as D-enantiomers), and KDO, with Neu5Ac present in the LPS but not in the liberated OH 4382-C2. FAB/MS for permethylated OH 4382-C2 (Figure 6) ions $[MCH_3]^+$ at *m/z* 1393 and 1394,[2] and $[M + H]^+$ (weak) at *m/z* 1322 corresponding to those of oligosaccharides with the respective compositions of Hex_2 Hep_2 PEA KDO and Hex_2 Hep_2 P KDO in the approximate ratio based on peak intensities of 5:1. Although linkage analysis (Table 3) indicated only Gal and Glc end groups and a 3-linked Hep residue, the appearance of a

[2] One or two ^{2}H atoms were incorporated into the CH_2 group of the KDO moiety due to enolization during ^2H_2O exchange for NMR analysis (see also Figure 7).

Table 3: Methylation Analysis of Core Oligosaccharides from O:19-Typed Isolate OH 4382

methylated sugar	molar ratios in oligosaccharides[a] OH 4382-C1	OH 4382-C2	OH 4382-C3
2,3,4,6-Me_4-Glc	1.0	1.1	1.2
2,3,4,6-Me_4-Gal		1.2	1.0
2,4,6-Me_3-Gal	1.1		
2,4,6,7-Me_4-Hep	1.0	1.0	1.0
2,6,7-Me_3-Hep			1.0
2,7-Me_2-Hep	+		
2,6-Me_2-Hep	+		
4,7,8,9-Me_4-Neu5Ac[b]	+		
4,7,9-Me_3-Neu5Ac[b]	+		

[a] Molar ratios are based on relative peak areas in GC/MS analyses of partially methylated alditol acetates and are normalized with respect to Hep residues. [b] Neu5Ac derivatives were identified by GC/MS of methyl ester methyl glycosides.

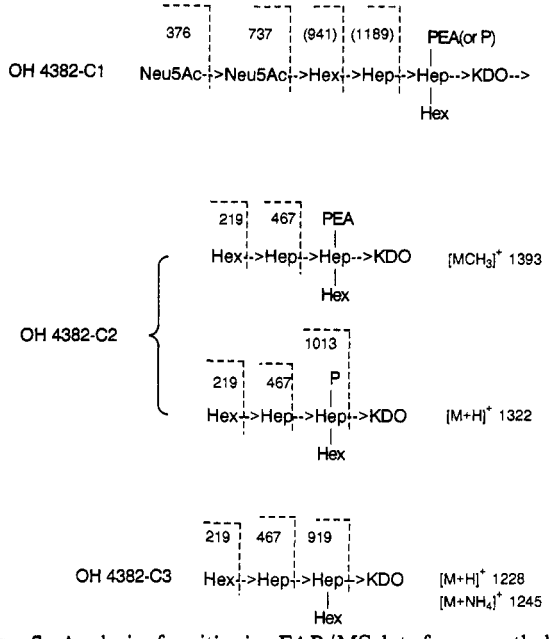

FIGURE 7: Analysis of positive ion FAB/MS data for permethylated core region in LPS from isolate OH 4382 and permethylated core OS derivatives. The ions in parentheses are tentative assignments.

fragment ion at m/z 1013 (Hex_2 Hep_2 P) from cleavage at the inner Hep residue, in addition to those at m/z 219 (Hex) and 467 (Hex Hep), was consistent with the presence of the minor molecular species. The main oligosaccharide component, although not showing a fragment ion from cleavage at the inner Hep residue, would presumably also carry attached Hex and phosphate (as PEA) moieties. The ^1H NMR spectrum of OH 4382 C2 showed only four anomeric proton signals, of which two at δ 5.36 (br s) and 5.09 (br s) were characteristic of Hep residues with the *α-manno* configuration and the other two at δ 4.87 ($J_{1,2}$ 7.5 Hz) and 4.56 ($J_{1,2}$ 8.5 Hz) could be tentatively assigned to β-Glc and β-Gal residues. A feature of note in the ^{13}C NMR spectrum was a methylene signal at δ 41.3 ($J_{C,P}$ 7 Hz) of the PEA moiety. These results clearly indicated that this core oligosaccharide, as reflected in the electrophoretic mobility of the low M_r LPS, was of shorter chain length than that of the O:19 reference strain.

O-Dephosphorylation by treatment of the core oligosaccharide with aqueous 48% HF furnished OH 4382-C3 for which FAB/MS of the permethylated derivative (data shown in Figure 7) showed protonated molecular ions at m/z 1228 and 1229[2] and ammonium adduct at m/z 1245 and 1246, corresponding to a single composition Hex_2 Hep_2 KDO, and

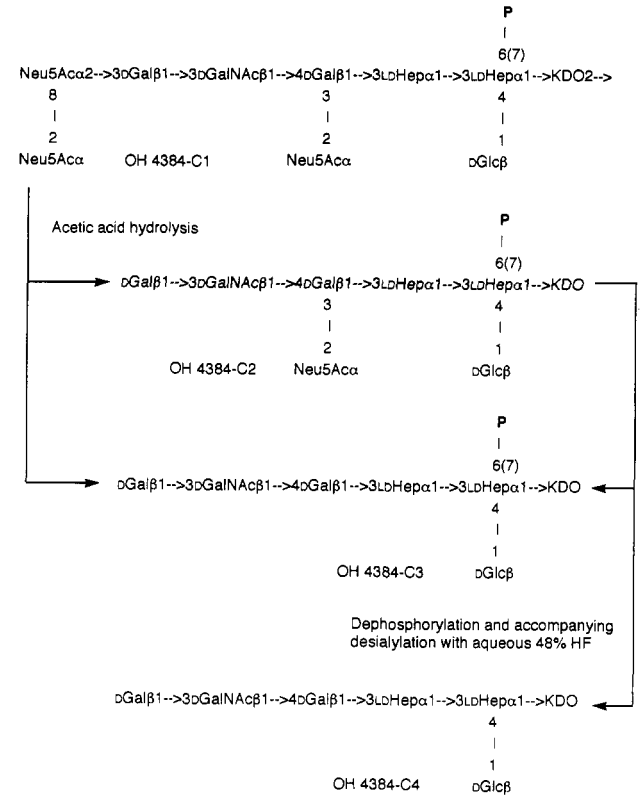

FIGURE 8: Genesis of fractions from LPS of isolate OH 4384, where struture OH 4384-C1 represents the most extended core OS chain in the intact LPS.

confirmed the removal of P and PEA moieties. The second Hep residue was not liberated on hydrolysis, and linkage analysis showed this to be a 3,4-branched unit (Table 3). The ^1H NMR spectrum confirmed the previous assignments of anomeric protons, but interestingly, the resonance formerly at δ 4.87 moved upfield on *O*-dephosphorylation so that the two β-Hex resonances for Glc and Gal at δ 4.55 and 4.56 could not be differentiated.

Since compositional analysis had shown Neu5Ac residues to be present in the low M_r LPS sample but absent from the liberated core oligosaccharide OH 4382-C2, the location of these acid-labile residues was achieved by careful examination of the *O*-deacylated LPS (designated as OH 4382-C1). FAB/MS (data shown in Figure 7) of permethylated OH 4382-C1 showed a series of fragment ions at m/z 376, 737, 941 (weak), and 1189 (weak) corresponding to a terminal sequence of Neu5Ac-Neu5Ac-Hex-Hep. Linkage analysis showed the presence of a 3-linked Gal residue and thus defined the site of attachment of a terminal Neu5Ac biosyl unit and confirmed the presence of the terminal Glc residue as a lateral side chain to the inner Hep residue. After dephosphorylation of permethylated OH 4382-C2, the qualitative detection of 2,7-(mainly) and 2,6-Me_2-Hep derivatives pointed to O-6 of the inner Hep residue as the main point of attachment of phosphate (P and PEA) units in the LPS. Linkage analysis was also conducted by methanolysis of permethylated OH 4382-C1, followed by acetylation and GC/MS analysis of the methylated Neu5Ac methyl ester methyl ketosides (Bhattacharjee & Jennings, 1976). The formation of 4,7,8,9-Me_4 and 8-Ac-4,7,9-Me_3 derivatives provided evidence for a 2→8 linkage in the Neu5Ac biose unit.

O-Deacylated LPS from Isolated OH 4384, Core Oligosaccharide, and Derivatives. The conclusions from structural investigations are summarized in Figure 8, which shows

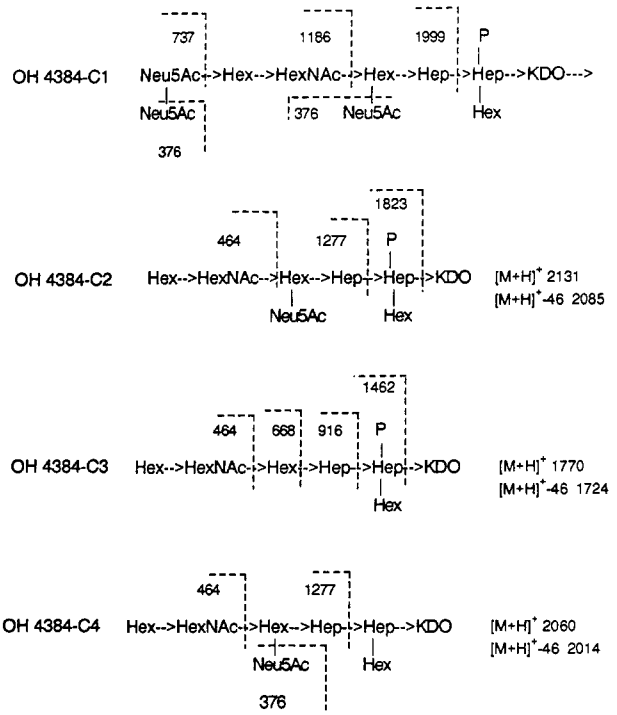

FIGURE 9: Analysis of positive ion FAB/MS data for permethylated core region in LPS from isolate OH 4384 and permethylated core OS derivatives.

Table 4: Methylation Analysis of Core Oligosaccharides from O:19-Typed Isolate OH 4384

	molar ratios in oligosaccharides[a]			
methylated sugar	OH 4384-C1	OH 4384-C2	OH 4384-C3	OH 4384-C4
2,3,4,6-Me_4-Glc	1.3	1.0	2.0	0.7
2,3,4,6-Me_4-Gal	0.6	0.8	1.5	1.0
2,3,6-Me_3-Gal	0.5	0.3	1.8	0.3
2,4,6-Me_3-Gal	0.6			
2,6-Me_2-Gal	1.2	1.2		1.1
2,4,6,7-Me_4-Hep	1.0	1.0	1.0	1.0
2,6,7-Me_3-Hep				1.0
4,6-Me_2-GalNAc	0.2	0.6		0.3
4,7,8,9-Me_4-Neu5Ac[b]	+			
4,7,9-Me_3-Neu5Ac[b]	+			

[a] Molar ratios are based on relative peak areas in GC/MS analyses of partially methylated alditol acetates and are normalized with respect to Hep residues. [b] Neu5Ac derivatives were identified by GC/MS of methyl ester methyl glycosides.

partial structures for *O*-deacylated LPS (designated as OH 4384-C1), liberated core oligosaccharides separated into the sialylated OH 4384-C2 and the corresponding asialo derivative OH 4384-C3, and the derivative OH 4384-C4 formed from OH 4384-C2 by *O*-dephosphorylation with some accompanying desialylation on treatment with aqueous 48% HF, FAB/MS data for permethylated OH 4384-C2 (Figure 9) showed protonated molecular ions $[M + H]^+$ at m/z 2131 and ($[M + H]^+ - 46$) at m/z 2085 (Dell et al., 1990), corresponding to a composition of Neu5Ac Hex_3 Hep_2 HexNAc P KDO. Linkage analysis (Table 4) showed similarity of structural units to those in the core OS **19**-C2 from the serostrain. Similarity in sequence was also indicated by the detection of fragment ions in FAB-MS at m/z 376 (Neu5Ac), 464 (Hex HexNAc), and especially at m/z 1277 corresponding to the branched structure Hex-HexNAc(Neu5Ac)-Hex-Hep for the outer core region. The presence of a phosphomonoester unit linked to the inner Hep residue was reflected in the observation of a glycosyloxonium ion in the FAB/MS at m/z 1823, whereas

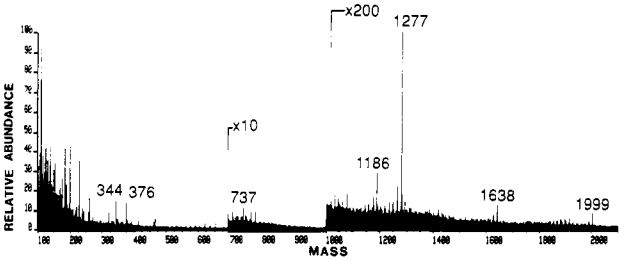

FIGURE 10: Positive ion FAB/MS spectrum of permethylated OH 4384-C1.

the corresponding ion arising from the cleavage at a Hep residue bearing a PEA moiety is not normally seen. These results may be accommodated in a core oligosaccharide structure for OH 4384-C2 that is identical, other than in the phosphate moiety, although unconfirmed in linkage differentiation at the inner Hep residue and its site of linkage to KDO, to that from the serostrain (OS **19**-C2). The minor core OS fraction OH 4384-C3 was shown to be a Neu5Ac-deficient derivative by the criteria FAB/MS (data shown in Figure 9) for the methylated derivative giving a protonated molecular ion at m/z 1770 and the ($[M + H]^+ - 46$) ion at m/z 1724, a series of fragment ions at m/z 464, 668, and 916 for a linear structure, and then an ion at m/z 1462 at the branched and phosphate-bearing inner Hep residue. This conclusion was supported by linkage analysis (Table 4) that reflected incomplete liberation of heptose but indicated the absence of branching at O-3 of the 4-linked Gal residue to which Neu5Ac had been attached. The ^1H NMR spectrum of OH 4384 C-2 was identical to that of OS **19** C-2 with signals for anomeric protons at δ 5.35 (br s) and 5.09 (br s) for the 2 Hep residues with the *α-manno* configuration, at δ 4.87 ($J_{1,2}$ 7.0 Hz) assigned to β-Glc, and at δ 4.71 ($J_{1,2}$ 8.5 Hz), 4.55 ($J_{1,2}$ 7.8 Hz), and 4.46 ($J_{1,2}$ 7.6 Hz) assigned to three β-Gal residues; resonances of the *N*-acetyl groups of GlcNAc and Neu5Ac residues were also observed as three-proton singlets at δ 2.08 and 2.07.

Evidence was also sought for the presence of additional Neu5Ac residues in the LPS that may have been lost during the liberation of core OS OH 4384-C2. Accordingly, as for the outer samples of low M_r LPS, the *O*-deacylated LPS, designated as OH 4384-C1, was prepared. FAB/MS of the permethylated derivative (Figure 10) showed a series of glycosyloxonium fragment ions of which those of highest mass could be considered to arise from cleavage at the outer of the two Hep residues. A structure is proposed in Figure 9 for the largest of these ions at m/z 1999 with the composition Hex_2 HexNAc Hep $Neu5Ac_3$. The detection of the fragment ion at m/z 1186 of composition Hex HexNAc $Neu5Ac_2$ was important in requiring that two of the three Neu5Ac residues were present in a disaccharide unit which linkage analysis showed was attached to O-3 of the outer Gal residue. This was in addition to the single laterally attached Neu5Ac residue linked to the inner Gal residue. The FAB/MS and linkage analysis data for OS 4384-C1 also provided evidence for the presence of outer chains that contained less than the full complement of Neu5Ac units. A chain deficient in the terminal Neu5Ac biose unit was implied by a series of ions that included those at m/z 464 (Hex HexNAc) and 1277 (Neu5Ac Hex_2 HexNAc Hep) and is consistent with the detection of terminal Gal residues in the preparation. Other chains carrying the Neu5Ac biose unit but deficient in the lateral Neu5Ac residue were indicated by the presence of some unbranched 4-linked Gal residues and a fragment ion at m/z 1638 of composition Hex_2 HexNAc Hep $Neu5Ac_2$.

As in the case of the LPS from the OH 4382 isolate, the Neu5Ac–Neu5Ac linkage was established by methylation analysis through the formation of 4,7,8,9-Me_4 and 8-Ac-4,7,9-Me_3 Neu5Ac derivatives. Insufficient material was available to determine the distribution of substituents at the inner Hep residue and its mode of linkage to the KDO residue.

DISCUSSION

In the examination of another of the 48 serotypically distinguishable strains of *C. jejuni*, the majority of which were judged by SDS–PAGE (Preston & Penner, 1987) to be of low M_r, the search was continued (Aspinall et al., 1992) for a structural basis for serological variations that could be accommodated in short oligosaccharide chains of ~8 residues of sugars of relatively common occurrence, Glc, Gal, LD-Hep, and GalNac, that were linked via KDO to the lipid A. In the case of the first group of lipopolysaccharides to be examined from serotypes O:1, O:4, O:23, and O:36, differences in sugar sequences and linkage types were sufficient to account for the serological differences. Striking results from these investigations were the discovery of Neu5Ac as a further constituent, although for these strains Neu5Ac was apparently not required to define serospecificity, and the recognition of structural similarities of the outer chains with those of gangliosides. In the present investigation the core region in the intact LPS of low M_r from *C. jejuni* serotype O:19 has been shown to consist of two closely related oligosaccharide types differing only in the presence or absence of a second Neu5Ac residue. One of the two closely related core structures for the O:19 LPS was indistinguishable from the predominant GD_{1a}-like disialo structure of the O:4 LPS, while the other O:19 core structure had a monosialo GM_1-like structure. It seems doubtful that the occurrence of the same two molecular species in only quantitatively different proportions, mainly the disialo and monosialo structures in approximately equal proportions in the O:19 LPS, provides a sufficient basis for serotypical discrimination, when this structural difference could result from incomplete biosynthesis or from inadvertent removal of Neu5Ac residues during chemical manipulations. Of potentially greater significance was the previous observation from SDS–PAGE, in conjunction with detection by immunoblotting with homologous and heterologous antisera, that there are structural differences in the O chain components of high M_r LPS of these two serotypes (Aspinall et al., 1993a). Adequate quantities for a detailed investigation of the high M_r LPS from the O:4 sterotype (Preston & Penner, 1987) have yet to be obtained, but that for the O:19 LPS is reported in the accompanying paper (Aspinall et al., 1994).

In parallel studies on LPS samples of low M_r from isolates typed as O:19, it was anticipated that structural similarities, if not complete identity, to LPS from the serostrain would be revealed. Of the samples of isolates from the two siblings, the core OS region of the isolate OH 4384 was closely similar but not identical to that of the O:19 serostrain. The glycosyl sequences in the O:19 LPS and the OH 4384 LPS were identical in the asialo core OS, but two points of differences were recognized. OH 4384 LPS showed variability in the extent of sialylation, but the sites of linkage at O-3 of terminal and internal 4-linked Gal residues were the same, although not always occupied. FAB/MS and linkage analysis data for the *O*-deacylated OH 4384 LPS showed that sialylation at the terminal residue was with a 2→8-linked neuraminobiose unit, a feature not observed in the serostrain LPS. Single Neu5Ac residues, or none, were present as lateral side chains at the internal Gal residue. Judged from the FAB/MS of

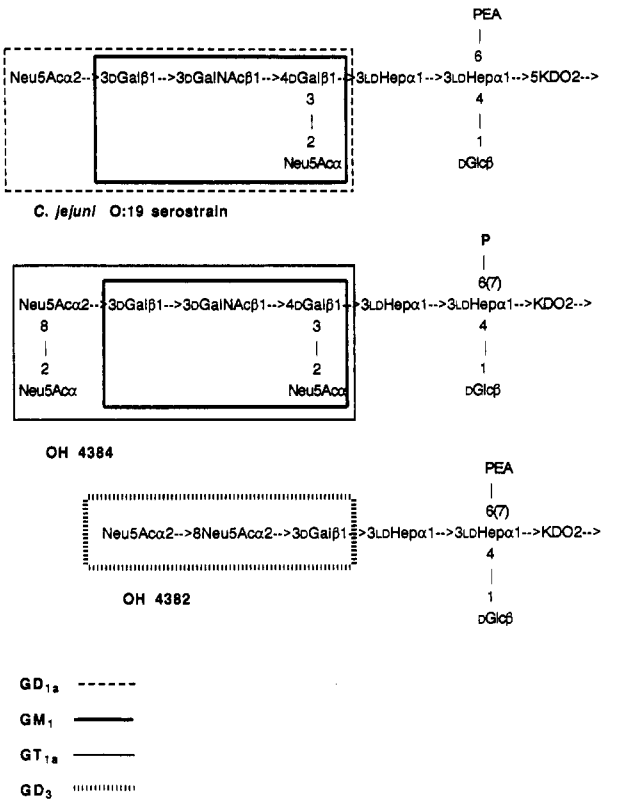

FIGURE 11: Outer regions of core OS structures from *c. jejuni* O:19 serostrain and isolates OH 4382 and OH 4384, showing homology with outer regions of gangliosides GD_{1a}, GM_1, GT_{1a}, and GD_3.

permethylated OS 4384-C1, the inner Hep residue was substituted by phosphate as a monoester in contrast to the more common phosphodiester, *O*-phosphoethanolamine (PEA), unit.

In contrast to LPS from the O:19 serostrain and the OH 4384 isolate, that from the OH 4382 isolate has been shown to contain a markedly shorter core OS unit lacking the terminal Gal and GalNAc residues of the former, and no evidence was seen for more complete oligosaccharide chains. Sialylation was with 2→8-linked neuraminobiose units and phosphorylation was mainly as PEA with a small amount as phosphomonoester.

There is a close relationship between the three core regions of low M_r O:19 LPS samples as well as that for O:4 since all contain external regions that mimic the corresponding regions of gangliosides (for a summary see Figure 11). A resemblance to GM_1 is only seen in some molecules of LPS from the O:19 serostrain and the OH 4384 isolate. A cross-reaction of the O:4 and O:19 LPS may be accounted for in the GD_{1a}-like regions but not in GM_1-like regions which, contrary to initial indications from examination of the liberated core oligosaccharide (Aspinall et al., 1992), are absent in the intact O:4 LPS (Aspinall et al., 1993b). There is a reasonable basis for the cross-reaction of low M_r LPS from O:4 with those of the O:19 serostrain and isolate OH 4384 but not for that of the shorter chain from isolate OH 4382, unless there are common epitopes in the inner core region. The outer region of the less extended low M_r LPS from OH 4384 does indeed mimic the outer region of GM_1 and that of the more extended chain mimics GT_{1a}, while the outer region of the low M_r LPS from OH 4382 mimics GD_3. Similarly, the reaction of the attenuated LPS of OH 4382 with rabbit anti-GM_1 antiserum remains unexplained unless there are small proportions of LPS with longer chains that have escaped detection.

These further examples of molecular mimicry of the ganglioside group of glycosphingolipids by LPS of low M_r from *C. jejuni* serotypes are strikingly similar to those of paraglobosides by the low M_r LPS (or so-called lipooligosaccharides) from *Neisseria* species, especially *Neisseria gonorrhoeae* (Gibson et al., 1989; John et al., 1991; Yamasaki et al., 1991a,b; Schneider et al., 1991).

Another unusual structural aspect of variable core regions in the O:19-related LPS preparations concerns the isolation of the *same* high M_r LPS from each sample. In the accompanying paper (Aspinall et al., 1994), the identical repeating structures in the O antigen chains have been established. The sites of attachment of the polysaccharide chains to *different* core regions have yet to be determined. To our knowledge this aspect of structure in LPS has been established unambiguously only for *Salmonella* spp. where advantage has been taken of the occurrence of SR mutants to furnish evidence that a wide variety of different O chains may be linked to a highly conserved core (Rietschel et al., 1990). In the present instance the observation of displaced ladderlike bands of similar periodicity, but slightly different mobilities, on SDS–PAGE suggests that identical O antigen chains may be linked to different core regions, with the further implication that analogous sites of attachment would be in inner regions of the core.

ACKNOWLEDGMENT

We are grateful to Dr. Ali Kandil for the provision of colominic acid as a reference substance for the linkage analysis for 2→8-linked Neu5Ac residues. We thank Dr. Jianyao Wang for recording some of the mass spectra on the ZAB spectrometer.

REFERENCES

Aspinall, G. O., McDonald, A. G., Raju, T. S., Pang, H., Mills, S. D., Kurjanczyk, L. A., & Penner, J. L. (1992) *J. Bacteriol. 174*, 1324–1332.

Aspinall, G. O., Fujimoto, S., McDonald, A. G., Pang, H., Kurjanczyk, L. A., & Penner, J. L. (1993a) *Infect. Immun.* (in press).

Aspinall, G. O., McDonald, A. G., Raju, T. S., Pang, H., Moran, A. P., & Penner, J. L. (1993b) *Eur. J. Biochem. 213*, 1017–1027.

Aspinall, G. O., McDonald, A. G., & Pang, H. (1994) *Biochemistry* (following paper in this issue).

Bhattacharjee, A. K., & Jennings, H. J. (1976) *Carbohydr. Res. 51*, 252–261.

Chen, P. S., Jr., Toribara, T. Y., & Warner, H. (1956) *Anal. Chem. 28*, 1756–1758.

Ciucanu, I., & Kerek, F. (1984) *Carbohydr. Res. 131*, 209–217.

Dell, A., Azadi, P., Thomas-Oates, J., Jennings, H. J., Beurret, M., & Michon, F. (1990) *Carbohydr. Res. 200*, 59–76.

Dubois, M., Gilles, K. A., Hamilton, J. K., Rebers, P. A., & Smith, F. (1956) *Anal. Chem. 28*, 350–356.

Gerwig, G. J., Kamerling, J. P., & Vliegenthart, J. F. G. (1978) *Carbohydr. Res. 62*, 349–357.

Gibson, B. W., Webb, J. W.; Yamasaki, R., Fisher, S. J., Burlingame, A. L., Mandrell, R. E., Schneider, H., & Griffiss, J. M. (1989) *Proc. Natl. Acad. Sci. U.S.A. 86*, 17–21.

Goldstein, I. J., Hay, G. W., Lewis, B. A., & Smith, F. (1965) *Methods Carbohydr. Chem. 5*, 361–370.

John, C. M., Griffiss, J. M., Apicella, M. A., Mandrell, R. E., & Gibson, B. W. (1991) *J. Biol. Chem. 266*, 19303–19311.

Kuroki, S., Haruta, T., Yoshioka, M., Kobayashi, Y., Nukina, M., & Nakanishi, H. (1991) *Pediatr. Infect. Dis. 10*, 149–151.

Moran, A. P., Zähringer, U., Seydel, U., Scholz, D., Stütz, P., & Rietschel, E. T. (1991) *Eur. J. Biochem. 198*, 459–469.

Penner, J. L., & Hennessy, J. N. (1980) *J. Clin. Microbiol. 12*, 732–737.

Penner, J. L., Hennessy, J. N., & Congi, N. V. (1983) *Eur. J. Clin. Microbiol. 2*, 378–383.

Preston, M. A., & Penner, J. L. (1987) *Infect. Immun. 55*, 1806–1812.

Pritchard, D. G., Rener, B. P., Furner, R. L., Huang, D. H., & Krishna, N. R. (1988) *Carbohydr. Res. 173*, 255–262.

Rietschel, E. T., Brade, L., Holst, O., Kulshin, V. A., Lindner, B., Moran, A. P., Schade, U. F., Zähringer, U., & Brade, H. (1990) in *Endotoxin Research Series*, Vol. 1. *Cellular and molecular aspects of endotoxin reactions* (Nowotny, A., Spitzer, J. J., & Ziegler, E. J., Eds.) pp 15–32, Excerpta Medica, Amsterdam, New York, Oxford.

Ropper, A. H. (1992) *New Engl. J. Med. 326*, 1130–1136.

Sawardeker, J. H., Sloneker, J. H., & Jeanes, A. (1967) *Anal. Chem. 37*, 1602–1604.

Schneider, H., Griffiss, J. M., Boslego, J. W., Hitchcock, P. J., Zahos, K. M., & Apicella, M. A. (1991) *J. Exp. Med. 174*, 1601–1605.

Walsh, F. S., Cronin, M., Koblar, S., Doherty, P., Winer, J., Leon, A., & Hughes, R. A. C. (1991) *J. Neuroimmunol. 34*, 43–51.

Westphal, O., & Jann, K. (1965) *Methods Carbohydr. Chem. 5*, 83–91.

Yamasaki, R., Bacon, B. E., Nasholds, W., Schneider, H., & Griffiss, J. M. (1991a) *Biochemistry 30*, 10566-10575.

Yamasaki, R., Nasholds, W., Schneider, H., & Picella, M. A. (1991b) *Mol. Immunol. 8*, 1233–1242.

York, W. S., Darvill, A. G., McNeil, M., Stevenson, T. T., & Albersheim, P. (1986) *Methods Enzymol. 118*, 3–40.

Yuki, N., Yoshino, H., Sato, S., & Miyataka, T. (1990) *Neurology 40*, 1900–1902.